2020 IEEE/ASME International Conference on
Advanced Intelligent Mechatronics (AIM), Boston, USA
(Virtual Conference), July 6-9, 2020

Analysis and Validation of Serpentine Locomotion Dynamics of a Wheeled Snake Robot Moving on Varied Sloped Environments*

Jason Lim[1], Weixin Yang[1], Yantao Shen[1], and Jingang Yi[2]

Abstract— **This paper investigates the problem of a multi-segmented and passively wheeled snake-like robot moving on varied sloped environments. The varied sloped environments indicate three-typical scenarios for the robot to move up, down and perpendicular to an incline in this investigation. The mathematical analysis of the motion dynamics for the snake robot moving in serpentine mode on the different sloped conditions is performed respectively, with a focus on how the motion dynamics change when the robot is on one of sloped environments as opposed to flat ground. The simulations based on these mathematical descriptions predict the effect of varying control parameters on the robot's motion on flat ground as well as motion up, down, and perpendicular to an inclined slope. Experiments confirm and validate results from the simulations. We found that an incline in the sloped environments affects not only the speed but also the direction of robot motion and degree of slipping at the friction points as well. These findings will help promote the design of task-oriented control strategies for steering the snake robot to move on a complex sloped environment.**

I. Introduction

Biomimetic robotics refers to robotic systems that mimic the structure or mechanisms of animals in order to achieve higher adaptability and other functional advantages that animals own over traditional robots. For example, snakes have several unique properties that make them intriguing to study for robotic applications. They are able to move in a wide variety difficult environments, can act as both locomotors and manipulators, and consist of an extremely simple, repeatable structure that is easy to scale to different sizes. Their compactness, versatility, and stability makes them potentially useful in many situations like disaster relief, search and rescue, planetary exploration, and other scenarios that require the navigation of complex terrains.

Previous researchers have identified several distinct types of snake locomotion gaits and developed corresponding dynamic and mathematical models to explain them. This paper focuses on a commonly used gait called lateral undulatory, or serpentine motion. During this motion a snake continually propagates an S-like curve along its body to slither forward, utilizing asperities in the surface environment and the frictional anisotropy of their scales to generate propulsive forces. Modular snake-like robots have been built to achieve lateral undulatory motion, often imitating the anisotropic friction property of snake scales with passive wheels that allow rolling in the tangential direction [1–6]. Other groups have shown it is possible to achieve serpentine locomotion using anistropic materials instead of wheels [7–9]. These snake-robots achieve locomotion by actuating the joints according to specific equations, and can be controlled autonomously by using feedback from sensors on the robot.

A majority of research into motion behavior and control strategies for the snake robot motion were conducted on flat ground. Several groups developed autonomous control schemes for tracking a reference trajectory on a flat surface [3, 10, 11]. Only a few groups have attempted to characterize and develop control strategies for snake robots' motion on sloped and varied environments. Endo identified the most important control parameter, the winding angle, for motion directly up a slope and proposed a control strategy to optimize this parameter [12]. Ma also studied the motion behavior of a snake robot moving up a slope, and simulation and experimental results showed the how the various control parameters affected the speed and ability to climb the slope [1]. Sato developed a decentralized control strategy to autonomously control a robot moving in a straight path on different surface environments and inclines [4]. A group at CMU proposed a method of controlling a different gait, sidewinding motion, to move on varying degrees of incline [9].

In this work we further investigate the problems of how motion dynamics change when a multi-segmented and passively wheeled snake-like robot moves in different directions on sloped environments in the serpentine motion gait. Previous work has assumed the motion stays in a straight path on the slope, but we investigate how both the speed and path of motion is affected by a slope. We explore the differences in motion on flat ground and motion directly up, down, and perpendicular to an incline. Both simulations and experiments are conducted to show the clear trends of how the incline affects the overall speed and direction of motion, as well as the degree of slipping in these different sloped environments. These revealing insights will certainly help adapt control strategies for steering snake robots to move on sloped and uneven environments.

II. Serpentine Locomotion Modeling

Several mathematical functions have been proposed to define the curve that a snake body follows during lateral undulatory motion. In this paper we use the Serpenoid curve

*This research was partially supported by the NSF Grant for REU Site in Biomimetics and Soft Robotics (BioSoRo) with Award Number EEC #1852578.

[1]Jason Lim, Weixin Yang, and Yantao Shen are with the University of Nevada, Reno, Electrical and Biomedical Engineering Department. jlim.kg@gmail.com, ytshen@unr.edu

[2]Jingang Yi is with Rutgers University, Mechanical and Aerospace Engineering Department. jgyi@rutgers.edu

defined by Ma in 2001, in which curvature varies sinusoidally as a function of arc length [1].

$$\kappa(s) = \frac{-2K_n\pi\alpha_0}{L} sin(\frac{2K_n\pi}{L}s), \tag{1}$$

where s, L, α_0, and K_n represent the arc length distance along the curve, total arc length, initial curve amplitude, and number of periods in the curve. For simplicity, in this paper $K_n = 1$ always. One can apply this equation to a segmented snake robot with n links, total length L, and link length of $L/n = \ell$ by integrating equation (1) to find the tangential angle of the i^{th} link, ϕ_i. Taking the difference of tangential angles of adjacent links will yield the following equation for relative joint angles, θ_i:

$$\theta_i(s) = -2\alpha_0 sin(\frac{K_n\pi}{n}) sin(\frac{2K_n\pi}{L}(s+i\ell)), \tag{2}$$

where $i = 1,..,n-1$. If the robot moves with constant velocity v_s along the curve, we can convert these equations to functions of time by making the substitution $s = s(t) = v_s t$ and simplify the joint angle equation to the following:

$$\theta_i(t) = \alpha sin(\omega t + \beta i) + \gamma, \tag{3}$$

where we have defined

$$\alpha \equiv -2\alpha_0 sin(\frac{Kn\pi}{n}),$$
$$\omega \equiv \frac{2Kn\pi}{L} v_s,$$
$$\beta \equiv \frac{2Kn\pi}{L} i.$$

In this paper, α will be referred to as the "winding angle parameter" or simply "winding angle", ω is the joint actuation angular frequency, β is the phase lag between relative joint angles, and γ is the heading parameter. As will be demonstrated by the simulation and experiment in sections IV and V, α and ω affect the shape and speed of the motion, and γ controls the direction of motion, with a value of 0 corresponding to straight forward motion.

III. Dynamics of Multi-segmented and Wheeled Snake Robot

A. Motion Dynamics

The snake robot is modeled as a series of n rigid links, each of length and mass ℓ and m. Each link is connected with actuators that allow for the control of the relative angle at the joints between links. Each link can subjected to a gravitational force, frictional forces, and constraint forces due to the other links. The friction force is assumed to be acting at a single point between the wheels on each link, as shown in Figure 2.

In reference to [1], it can be shown that applying the Newton-Euler equations to the force model, and generalizing the equations to n links, the robot dynamics can be arranged into the following equations:

$$\mathbf{D\tau} = {}^f\boldsymbol{\tau} + {}^0\boldsymbol{\tau} + \mathbf{M_0}\ddot{\mathbf{p}}_\mathbf{0} + \mathbf{M}\ddot{\boldsymbol{\phi}} \tag{4}$$
$${}^f\mathbf{f} + {}^0\mathbf{f} + \mathbf{m_0}\ddot{\mathbf{p}}_\mathbf{0} + \mathbf{m}\ddot{\boldsymbol{\phi}} = \mathbf{0}, \tag{5}$$

for motion on flat ground, and

$$\mathbf{D\tau} = {}^f\boldsymbol{\tau} + {}^0\boldsymbol{\tau} + \mathbf{M_0}(\ddot{\mathbf{p}}_\mathbf{0} + \mathbf{g}) + \mathbf{M}\ddot{\boldsymbol{\phi}} \tag{6}$$
$${}^f\mathbf{f} + {}^0\mathbf{f} + \mathbf{m_0}(\ddot{\mathbf{p}}_\mathbf{0} + \mathbf{g}) + \mathbf{m}\ddot{\boldsymbol{\phi}} = \mathbf{0}, \tag{7}$$

for motion on an incline, where the position of the tail and shape of the robot are defined by $\mathbf{p}_0$ and ϕ. Equations (4) and (6) are n-dimensional systems of equations relating the forces on each link to the robot's shape and motion. These equations can be combined to yield equation (8), which allows the joint torques and accelerations to be solved from equation (2). The full definitions of all variables are given in [1].

The effect of an incline on the robot dynamics is mathematically apparent in the gravitational acceleration vector, $\mathbf{g}$ (whose definition depends on the three motion scenarios as shown in Figure 1), which adds an additional external force to the dynamics. In order to solve for the robot's motion, an initial position, orientation, and the shape variables in equation (2) must be prescribed. The motion of the whole robot can then be derived through numerical integration. The motion can also be derived through prescribing the joint torques, τ, and an initial position.

$$\mathbf{D\tau} + (\mathbf{M_0}\mathbf{m_0^{-1}}\mathbf{m} - \mathbf{M})\mathbf{e}\ddot{\phi}_0 =$$
$${}^f\boldsymbol{\tau} + {}^0\boldsymbol{\tau} - \mathbf{M_0}\mathbf{m_0^{-1}}({}^f\mathbf{f} + {}^0\mathbf{f}) + (\mathbf{M_0}\mathbf{m_0^{-1}}\mathbf{m} - \mathbf{M})\mathbf{E}\ddot{\theta} \tag{8}$$

B. Friction Model

Most models for analyzing lateral undulatory motion for snake robots with passive wheels assume that the wheels do not slip in the normal direction. For our robot, slipping occurs often and the amount of slipping varies for different motion parameters and environmental factors, significantly affecting the motion characteristics. Therefore a friction model that includes both static and dynamic friction to accurately model slipping at the friction points is necessary for our studies. Based on Ma [13], the following friction model includes both static and dynamic friction, basing the transition from one to the other on a threshold velocity, V_{Th}:

$${}^f f_i^\lambda = \begin{cases} \frac{-v_i^\lambda}{V_{Th}} \mu_s^\lambda F_N i & |v_i^\lambda| < V_{Th} \\ -sign(v_i^\lambda)\mu_d^\lambda F_N i & |v_i^\lambda| \leq V_{Th} \end{cases}, \tag{9}$$

where $\lambda = t,n$ differentiates between tangential and normal directions, v_i^λ is the speed of the friction point in the tangential or normal direction, μ_s^λ and μ_d^λ are the static and dynamic coefficients of friction, respectively, and F_{Ni} is the normal force of link i, defined as

$$F_{Ni} = m_i g cos(\psi) \tag{10}$$

for motion on an incline of angle ψ. The net x and y friction forces can then be written as follows:

$${}^f f_i^x = {}^f f_i^t cos\phi_i - {}^f f_i^n sin\phi_i, \tag{11}$$

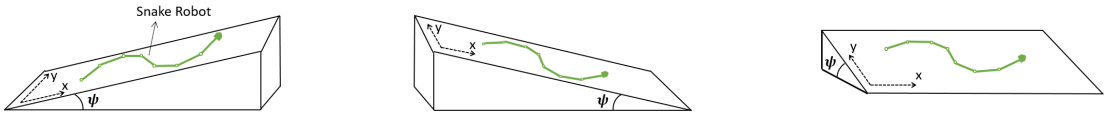

(a) Motion up an incline, $\mathbf{g} = [gsin\psi \quad 0]^T$

(b) Motion down an incline, $\mathbf{g} = [-gsin\psi \quad 0]^T$

(c) Motion perpendicular to an incline, $\mathbf{g} = [0 \quad gsin\psi]^T$

Fig. 1. Three different motion scenarios will be studied for an incline of degree ψ. Coordinate setup is shown for each scenario, where the definition of $\mathbf{g}$ will depend on each scenario ($g = 9.8N$).

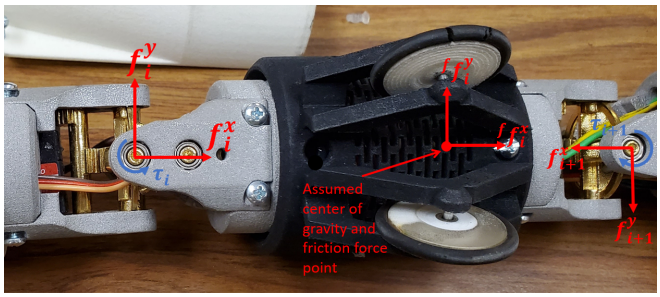

Fig. 2. Snake robot link showing the assumed center of mass and single friction contact point, along with external forces acting on link.

$$^f f_i^y = {}^f f_i^t sin\phi_i + {}^f f_i^n cos\phi_i. \tag{12}$$

In this model the friction forces themselves are only affected by an incline through a reduction of the normal force exerted by the mass of the robot. The maximum static friction force is therefore reduced, making slipping at the friction points more likely to occur. The robot motion will also be affected by the additional gravitational force acting down the slope.

The static friction coefficients of our snake robot were measured by using a force sensor to detect the force at which the robot started to move, and the dynamic coefficients were found by measuring the force necessary to pull the robot at a constant velocity. As the threshold velocity V_{Th} is difficult to measure, it is estimated by tuning the simulation to most closely match the actual robot behavior.

IV. Simulating Robot Motion on Slopes

TABLE I

Simulation Parameters

n	8
m_i	0.157 kg
ℓ_i	0.1325 m
ℓ_{Gi}	$\ell_i/2$
ℓ_{fi}	$\ell_i/2$
μ_s^n	0.8
μ_d^n	0.5
μ_s^t, μ_d^t	0.085
V_{Th}	0.05 m/s
step size	0.005 s
simulation time	8 s

To investigate the motion characteristics of the snake robot for three different ideal situations, motion directed up, down, and perpendicular to an incline, a simulation is conducted based on the models defined in sections II and III. Table I shows the parameters used in our simulation, which are

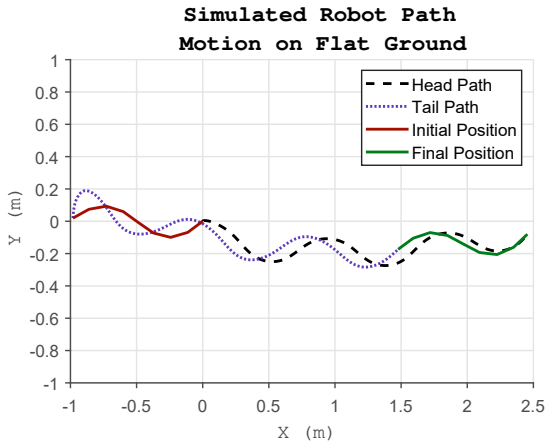

Fig. 3. Simulated robot path for motion on flat ground demonstrates how the robot moves in a straight path when no incline is present.

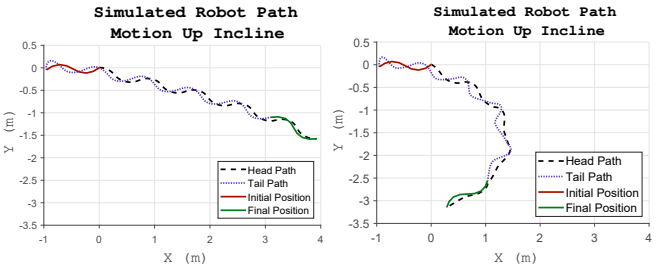

(a) $\psi = 2°$ (b) $\psi = 4°$

Fig. 4. Simulated robot paths for motion up an incline demonstrate how the direction of motion is affected by an incline. A larger incline affects the direction more significantly.

the best estimate of the true values of our robot in the experiment.

The position of the robot must be obtained by integrating $\ddot{\mathbf{p}}_0$ and $\ddot{\phi}$, which is difficult to solve analytically since almost all of the terms in the force and torque equations depend on $\dot{\phi}$ and ϕ. However using Euler's method of numerical integration the entire motion can be estimated from an initial position and joint velocity, assuming the robot maintains the prescribed serpentine shape given by equation (2) or (3). The following describes the algorithm for a Python simulation used to plot the robot's trajectory:

1) Prescribe specific serpenoid shape parameters, $\theta(t)$, and initial conditions $\dot{\phi}(t=0)$, $\phi(t=0)$, $\dot{\mathbf{p}}_0(t=0)$, and $\mathbf{p}_0(t=0)$.
2) Calculate $\ddot{\mathbf{p}}_0(t=0)$ and $\ddot{\phi}(t=0)$ using equation (5) or

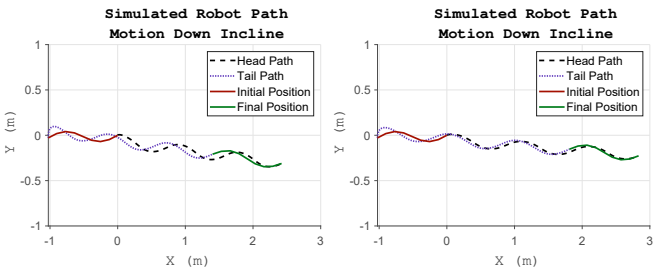

(a) $\psi = 2°$ (b) $\psi = 4°$

Fig. 5. Simulated robot paths for motion down an incline demonstrate how the direction of motion is not significantly affected in this case, however the speed is increased for a larger incline as evidenced by the farther travel distance.

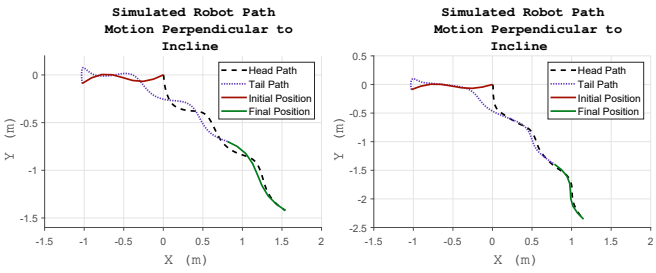

(a) $\psi = 2°$ (b) $\psi = 4°$

Fig. 6. Simulated robot paths for motion perpendicular to an incline demonstrate how the motion path gets directed down the incline, and more severely for larger inclines.

(7), and equation (8). The joint torques, τ can also be calculated.

3) Choosing a small time step δt, use Euler's method to calculate $\dot{\phi}(t = \delta t)$, $\phi(t = \delta t)$, $\dot{\mathbf{p}}_0(t = \delta t)$, and $\mathbf{p}_0(t = \delta t)$ from $\ddot{\mathbf{p}}_0(t = 0)$ and $\ddot{\phi}(t = 0)$. The rest of the robot's position is obtained using the relative joint angles.
4) Continue repeating steps 2-3 at the next time step, thus deriving the whole robot motion.

Note that this method only gives an estimation of the resulting motion characteristics, thus the main results of the simulation should be considered qualitatively, rather than quantitatively. As expected, the speed of the robot moving up an incline is decreased compared to flat ground under the same control parameters, but the direction of motion also gradually shifts, as seen by comparing Figure 3 with 4 and 6. The same goes for motion directed perpendicular to the incline, suggesting that the heading parameter γ will have to be actively controlled to maintain moving in a straight line on an incline, an important distinction from flat ground motion. For motion directed down an incline, the speed is affected, but the direction of motion is not as significantly affected as for motion up or perpendicular to the incline. The simulation also predicts that for locomotion to be possible up an incline a minimum and maximum value exists for the winding angle parameter α that is closely related to the degree of incline. The friction coefficients also greatly affect the ability to move on both flat ground and an incline; if the normal friction coefficient is too low, motion is not even possible.

Figure 7a, 7c, and 7e show the average transverse velocity for different winding angles predicted by the simulation. These plots show clear trends for the motion characteristics, that is, when moving up an incline, the speed increases with increasing winding angle until a certain point, where the speed drops again. For motion down an incline however, as the winding angle parameter increases, the speeds converge to a certain value. For motion perpendicular to an incline, the path direction is shifted down the slope, causing the rate of increase in speed to fall with larger inclines.

V. Experimental Validation

Using a prototype snake robot built from 3D printed parts, experimental tests are conducted to confirm and quantify the results of the simulation. Passive rubber-ringed wheels are used on the bottom of each link of the robot, and the tests are conducted on a flat wooden platform set at different inclines. A video tracking software is used to trace the robot's motion and measure the average velocity. The robot is operated by a micro-controller program that actuates each joint according to the pattern in equation (3), and tests are performed for various values of the winding angle parameter α and joint angular frequency ω, defined in equation 3.

Experiments confirm that the speed of the robot can be varied by changing α and ω. An incline will not only affect the speed of the robot but also gradually shift the direction of motion, as shown by the sequential snapshots in Figure 8. Tests also confirm that a lower limit for the winding angle parameter exists in order for the robot to move uphill, and this lower limit correlates positively with the degree of incline. Figures 7b, 7d, and 7f show the effect of the winding angle on average transverse speed for various degrees of incline for the three motion scenarios, which correspond with the simulation results in Figures 7a, 7c, and 7e. On flat ground, motion is possible over a wide range of α values, but this range of acceptable values gets smaller for motion up an incline. For motion down an incline, the average speed converges to a certain value with increasing α. For motion perpendicular to the incline, the average speed on inclined environments is increased for small winding angles, but decreases quickly as the winding angle increases. One fact realized by the experiments is that the degree of slipping at the friction points is greatly affected by the incline, especially for motion up and perpendicular to the incline. Because the transition from static to dynamic friction is difficult to model in this situation, the degree of slipping is a major cause for the discrepancies between the simulation and experimental data. Additionally, the real joint angles and angular velocity do not exactly track their reference values, especially when a large degree of slipping occurs. The error and noise in the joint actuation is another major cause for disagreements between the simulation and experiment.

VI. Conclusion and Future Work

The goal of this research is to investigate the locomotion mechanisms of multi-segmented and passively wheeled

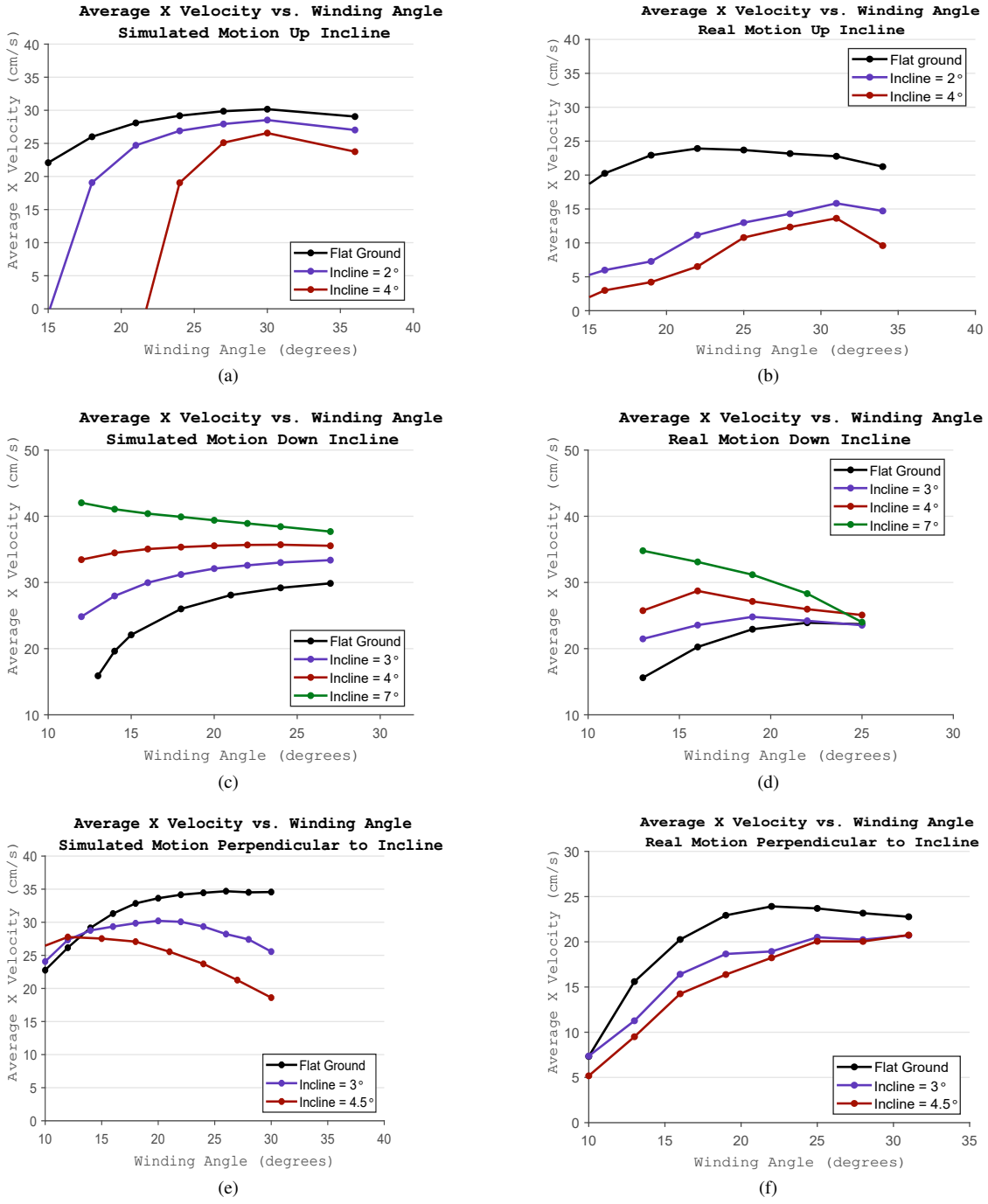

Fig. 7. Plots are shown for average velocity in the x direction vs. winding angle for different degrees of incline for the three cases of motion, up, down, and perpendicular to the slope. While there are numerical discrepancies between the simulation and experiment, the simulation data shows certain overall trends that are validated by the experimental data.

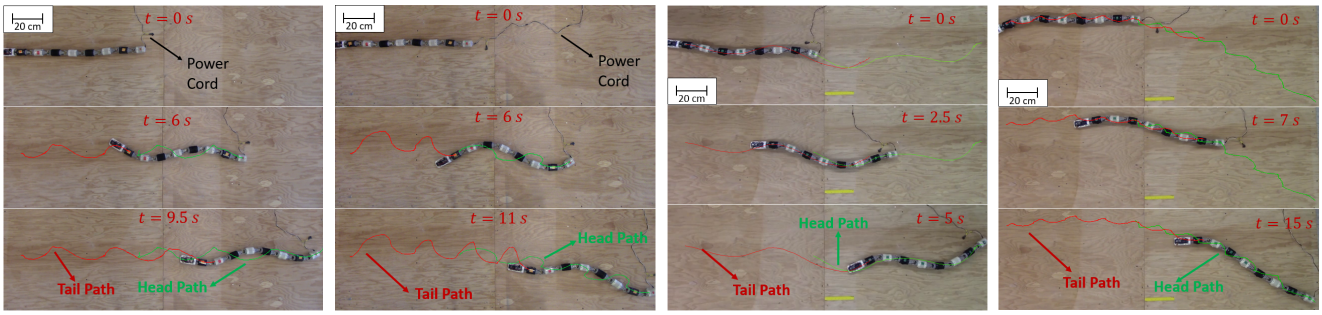

(a) Motion on flat ground. ($\psi = 0°$) (b) Motion up an incline. ($\psi = 2°$) (c) Motion down an incline. ($\psi = 3°$)(d) Motion perpendicular to an incline. ($\psi = 3°$)

Fig. 8. A video tracking software is used to trace the robot's motion, yielding the green and red curves corresponding to the robot's head and tail trajectories. The four different scenarios shown are motion on a flat surface (8a), motion up an incline (8b), motion down an incline (8c), and motion perpendicular to an incline (8d). Tests show that the average speed, body shape, and direction of the motion can be affected by a small incline. The incline also significantly affects the degree of normal slipping at the friction points, which is one of the main factors that influence the change in speed and direction of the robot.

snake-like robots and characterize the robot's motion on varied sloped environments. The snake-like robot is able to achieve serpentine locomotion by actuating the relative joint angles according to a simple mathematical description. Analysis of the physical behaviors reveals that an incline will affect the motion by introducing an external gravitational force and reducing the maximum frictional force.

The simulations based on the dynamic models predict how the motion is affected by an incline and varying different control parameters, and experimental tests confirm and quantify the motion characteristics. Results show that the speed of the robot depends on the control parameters ω, the relative joint angular frequency, and α, the winding angle parameter, as well as the friction coefficients between the robot and the surface environment. The robot's path direction can be controlled with γ and is affected by an incline. The average speed moving up an incline decreases significantly as expected. For motion up and perpendicular to an incline, the direction of motion is shifted and slipping occurs more often due to the additional gravitational force. A threshold of values exist for α that allow motion to be possible, and this threshold depends heavily on the degree of incline. These findings agree with previous research [1, 12].

The results from the simulation and experiments provide insight towards developing a solution for controlling the robot's speed and direction on an uneven environment. On flat ground the robot can track a reference position and velocity by actively controlling just ω and γ [10, 11]. On an incline, however, the speed and direction also heavily rely on α, which means α should also be considered in the control strategy. Another reason to include α, and even β, in the control strategy is that these parameters are the primary factors that determine efficiency of the motion [7], making it advantageous to adjust these parameters to track their optimal values.

The future goals of this research are to improve the simulation model to better incorporate the dynamics of slipping, and to collect more data on the motion characteristics of the snake robot on combined sloped environments or irregular terrain surfaces, so as to design advanced control strategies that allow the robot to track a position and velocity on a complex sloped environment and irregular terrains as well.

REFERENCES

[1] S. Ma, N. Tadokoro, B. Li, and K. Inoue, "Analysis of creeping locomotion of a snake robot on a slope," *2003 IEEE International Conference on Robotics and Automation*, pp. 15–23, 2003.

[2] S. Hirose and H. Yamada, "Snake-like robots," *IEEE Robotics Automation Magazine*, vol. 16, no. 1, pp. 88–98, 2009.

[3] F. Matsuno and H. Sato, "Trajectory tracking control of snake robots based on dynamic model," *Proceedings of the 2005 IEEE International Conference on Robotics and Automation*, pp. 3029–3034.

[4] T. Sato, T. Kano, and A. Ishiguro, "A decentralized control scheme for an effective coordination of phasic and tonic control in a snake-like robot," *Bioinspiration Biomimetics*, vol. 7, no. 1, pp. 1–9, 2011.

[5] A. Crespi and A. Ijspeert, "Online optimization of swimming and crawling in an amphibious snake robot." *IEEE Transactions on Robotics*, vol. 24, pp. 75–87, 2008.

[6] M. Nakajima, M. Tanaka, K. Tanaka, and F. Matsuno, "Motion control of a snake robot moving between two non-parallel planes," *Advanced Robotics*, vol. 32, pp. 1–15, 2018.

[7] M. Saito, M. Fukaya, and T. Iwasaki, "Serpentine locomotion with robotic snakes," *IEEE Control Systems*, vol. 22, no. 1, pp. 64–81, 2002.

[8] T. Kano, T. Sato, R. Kobayashi, and A. Ishiguro, "Decentralized control of scaffold-assisted serpentine locomotion that exploits body softness," *2011 IEEE International Conference on Robotics and Automation*, pp. 5129–5124, 2011.

[9] C. Gong, M. Tesch, D. Rollinson, and H. Choset, "Snakes on an inclined plane: Learning an adaptive sidewinding motion for changing slopes," *2014 IEEE/RSJ International Conference on Intelligent Robots and Systems*, pp. 1114–1119, 2014.

[10] G. Wang, W. Yang, Y. Shen, H. Shao, and C. Wang, "Adaptive path following of underactuated snake robot on unknown and varied frictions ground: Theory and validations," *IEEE Robotics and Automation Letters*, vol. 3, no. 4, pp. 4273–4280, 2018.

[11] E. Kelasidi and A. Tzes, "Serpentine motion control of snake robots for curvature and heading based trajectory - parameterization," *2012 20th Mediterranean Conference on Control Automation (MED)*, pp. 536–541, 2012.

[12] G. Endo, K. Togawa, and S. Hirose, "A self-contained and terrain-adaptive active cord mechanism," *Advanced Robotics*, vol. 13, no. 1, pp. 243–244, 1999.

[13] S. Ma, Y. Ohmameuda, and K. Inoue, "Dynamic analysis of 3-dimensional snake robots," *2004 IEEE/RSJ International Conference on Intelligent Robots and Systems (IROS)*, pp. 767–772, 2004.